**LOADING ON FUEL RODS IN A SURROGATE
PWR ASSEMBLY SUBJECTED TO SIMULATED
NORMAL CONDITIONS OF TRUCK TRANSPORT**

Paul McConnell
Sandia National Laboratories

Doug Ammerman   **Ken Sorenson**
Sandia National Laboratories   Sandia National Laboratories

ABSTRACT
This paper describes a test performed to directly measure loads imparted to fuel rods in a fuel
assembly subjected to conditions of normal truck transport. The motivation for the test was 1)
fuel rods will be subjected to higher burn-up and potentially long periods of storage before
transport - mechanisms that may embrittle the cladding, and 2) there is a paucity of experimental
data for loads measured directly on fuel rods under transport conditions.
A PWR assembly with surrogate fuel rods was subjected to vibration and shock profiles
simulating normal transport within a truck cask. The vibration and shock profiles were derived
from data available in the open literature obtained by measuring accelerations on actual truck
casks. These profiles served as input to a shaker on which the fuel assembly within a basket was
attached simulating the configuration of an assembly within a truck cask. Selected fuel rods were
instrumented with accelerometers and strain gauges to derive the loads on the rods imparted by
peak vibrations and shocks.
The test results are reported and related to analytical results from finite element modeling. The
results are also discussed in terms of potential implications of the transport of embrittled fuel-rod
cladding.

INTRODUCTION
Long-term storage and subsequent transportation of high-burnup used nuclear fuel (UNF) is an
issue requiring quantitative knowledge of UNF material properties and its response to
mechanical loadings during transport. The fuel clad is the first line of defense for containment of
the used nuclear fuel; therefore, it is important to understand if cladding can maintain its integrity
during normal conditions of transportation.
The normal conditions of transport are those defined within the United States Nuclear
Regulatory Commission (US NRC) regulations in 10 Code of Federal Regulations (CFR) Part 71
[1] and the International Atomic Energy Agency SSR-6 regulations [2].
Specifically, the regulations require packages for transporting UNF to meet conditions defined in
10 CFR Part 71.71 during normal transport. The effect of "vibration normally incident to
transport" must be determined for a package design (§71.71(c)(5)). The NRC also provides

guidance in §2.5.6.5 *Vibration* in the "Standard Review Plan for Transportation Packages for Radioactive Material", US NRC NUREG-1609 [3], which also cites NUREG/CR-0128 and NUREG/CR-1277 [4-5]. These documents include information on shock loadings and random vibration.
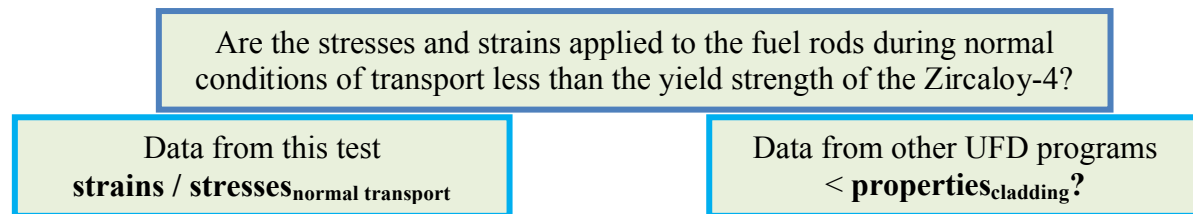
PURPOSE

This test program was designed to better understand fuel rod response to *normal* conditions of truck transport (NCT) loadings in order to estimate the ability of aged, used nuclear fuel to withstand these conditions. The experimental work was focused on testing a 17×17 PWR assembly containing instrumented surrogate fuel rods (Figure 2) placed upon a shaker (Figure 3) to simulate vibrational and shock loading associated with a normal 700-mile truck journey.

The data from the tests described herein shall be compared to data to be generated in other DOE Used Nuclear Fuel Disposition Campaign separate effects testing activities to obtain mechanical properties of high-burnup and aged UNF. Comparing the strains applied to fuel cladding during NCT to the strength of UNF enables an assessment of the ability of the cladding to withstand post-storage transportation environments. The data from these tests shall also be used to validate finite element models used to predict the behavior of aged, high-burnup fuel under normal conditions of transport.

The data needed to help predict whether aged, high-burnup fuel can withstand normal conditions of transport falls in two categories: 1) the loads imposed directly on rods during NCT (the scope of this report); and 2) the material properties of aged, high-burnup cladding (outside the scope of this report). Fuel rods subjected to high burnups *may* be sufficiently embrittled such that loads applied to the rods during normal transport *could* result in rod failure.

Zircaloy-4 cladding burned to high levels will likely experience an increase in yield strength with a significant decrease in ductility. Brittle fracture of high-burnup Zircaloy-4 could occur at applied stresses approaching the yield strength of the material. High-burnup Zircaloy-4 may also be below the ductile-to-brittle transition temperature at temperatures associated with long-term dry storage and subsequent transport of used fuel. This implies that the alloy will be at its "lower shelf" and susceptible to brittle fracture. Unirradiated and low-burnup (to a to-be-determined burnup level) Zircaloy-4 likely exhibits ductility at stress levels beyond the yield strength and is less susceptible to brittle fracture.

The margin of safety between the applied loads on fuel rods and the material properties of the high-burnup rods has not been quantified. So, a relevant question is,

> Are the stresses and strains applied to the fuel rods during normal conditions of transport less than the yield strength of the Zircaloy-4?

Data from this test	Data from other UFD programs
strains / stresses$_{\text{normal transport}}$	< **properties**$_{\text{cladding}}$?

OBJECTIVES OF THE TEST

The objectives of this test program were to:

- Simulate over-the-road tests on a full-scale surrogate fuel assembly by applying loadings to fuel cladding that would be experienced during normal conditions of truck transport.
- Instrument the cladding to capture accelerations and strains imposed by the mechanical loadings resulting from the normal condition of transport vibrations and shocks.

- Provide a data point– applied strain/stress$_{normal\ transport}$ - related to the issue of the margin of safety to understand if there is an immediate concern about the ability for aged, used fuel to withstand normal conditions of transport.

BASIS OF TEST
The *ideal test* would be to place an *irradiated fuel assembly* in an *actual cask* and do *over-the-road/rail tests* to measure the vibrational and shock response of the rods to the transport conditions. But, performing such a test with an irradiated assembly would be costly and instrumenting high-burnup cladding would result in high personnel radiation exposures.
An alternative solution is to use an *unirradiated assembly* in an *actual cask*. However, no rail casks are available, only truck casks with internal contamination because they have all been in reactor pools.
Due to these conditions, the test plan took the practical alternative to place an unirradiated fuel assembly using surrogate rod materials on a shaker and subject the assembly to vibrations and shocks simulating normal transport via a truck cask. Three of the tubes were Zircaloy-4 – these rods were instrumented- and the remaining tubes were copper. All the tubes contained a lead rod which simulated the UO_2.
Compromises were required in the test design. Table 1 identifies components of an ideal test, constraints to these components, and the compromises made to develop the final test configuration.

Table 1. Constraints and compromises for the shaker assembly test

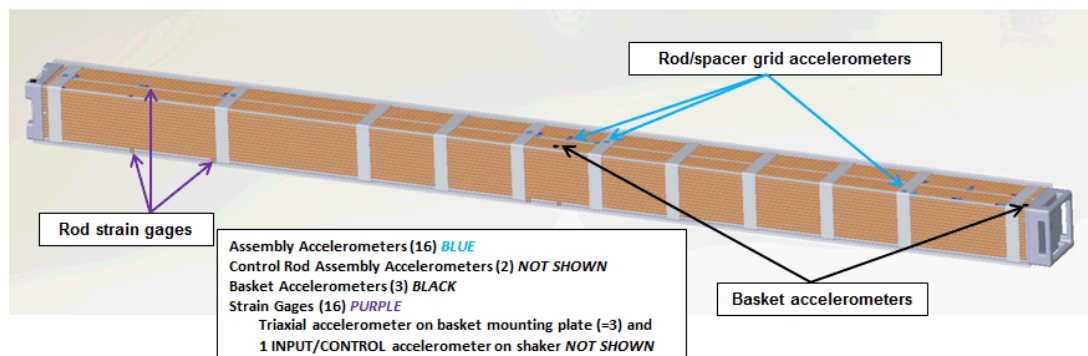| Ideal Experimental Design	Constraint	Compromise Solution for Test	Comments
Use actual cask	• Available truck casks contaminated • Rail casks unavailable	Simulate truck transport with a shaker	Applicable shock/vibration data available from NUREG/CR-0128
Use actual PWR assembly	Use of an irradiated assembly not feasible	PWR assembly was available	
Use zirconium alloy rods	Limited number of Zircaloy-4 rods available	• Use copper alloy tubes for most assembly locations • Use Zircaloy-4 rods for those rods to be instrumented	Among many materials evaluated for surrogates for Zircaloy-4 and UO_2, copper and lead had best combination of material properties (elastic modulus and density, respectively), availability, and cost
Use UO_2 pellets in rods	UO_2 pellets unavailable	Use lead rods as surrogate	
Rods have same material properties as used in an actual assembly	• Limited number of Zircaloy-4 rods available • UO_2 pellets unavailable	• Adjust wall thickness of copper tubes so that $EI_{Cu} \approx EI_{Zircaloy-4}$ • Adjust amount of lead in tubes so total assembly weight is that of an actual assembly	

| Ideal Experimental Design	Constraint	Compromise Solution for Test	Comments
Assembly is in an actual basket which is within a cask	Actual basket unavailable	Construct a basket to contain assembly	
Basket within a truck cask has some freedom of motion	Experimentally unviable to allow basket to move shaker due to shaker control constraints	Attach basket to shaker to prevent motion	
Assembly in basket has freedom of motion	None	Fuel assembly allowed same freedom of motion as an assembly within an actual NAC-LWT PWR basket	Within the basket, the assembly had 0.45 in. (1.14 cm) clearance at the top and 0.225 in. (0.57 cm) along the sides
Assembly subjected to actual truck transport environment	Truck cask unavailable	Derive inputs for shaker from truck vibration/shock data	• Vibration data and shaker inputs ranged from 5 Hz to 2,000 Hz • Shock data ranges from 0.5 Hz to 420 Hz. Shaker inputs for shock ranged from 4 Hz to 600 Hz
Basket/ assembly within an actual truck cask	Truck cask unavailable	• Basket constructed to conform to material (aluminum), weight, and internal dimensions of NAC-LWT PWR basket • Basket affixed to shaker	
Instrument assembly and basket (accelerometers and strain gages)	None	• Apply expert judgment and analyses to define location of instruments • Instrument selected rods	• All rods are expected to respond in a similar manner (per analyses) • Used 16 strain gages and 25 accelerometers

TEST PARAMETERS

Instrumentation

Modeling an assembly identified the optimum locations for the instrumentation [6], with Zircaloy-4 rods placed at the top, middle rod location; a top, side location; and the bottom, side location below the top, side Zircaloy-4 rod. Instrumentation was placed at various locations on these three rods at the midpoint between spacer grid supports and adjacent to the spacer grids to provide a representative profile of the loading on the rods.

Strain gages were placed on the cladding to measure strains during the tests. Accelerometers were placed at strategic locations on the shaker, basket, assembly spacer grids, and selected rods (Figure 1). The tests employed 16 strain gages and 25 accelerometers.

Rod/spacer grid accelerometers

Rod strain gages

Assembly Accelerometers (16) *BLUE*
Control Rod Assembly Accelerometers (2) *NOT SHOWN*
Basket Accelerometers (3) *BLACK*
Strain Gages (16) *PURPLE*
    Triaxial accelerometer on basket mounting plate (=3) and
    1 INPUT/CONTROL accelerometer on shaker *NOT SHOWN*

Basket accelerometers

Figure 1. Location of instrumentation on assembly/basket for shaker tests. There were three Zircaloy-4/lead rods and 261 copper/lead rods.

Figure 2 shows the location of the Zircaloy-4 rods which were instrumented and instrumentation of the actual assembly.
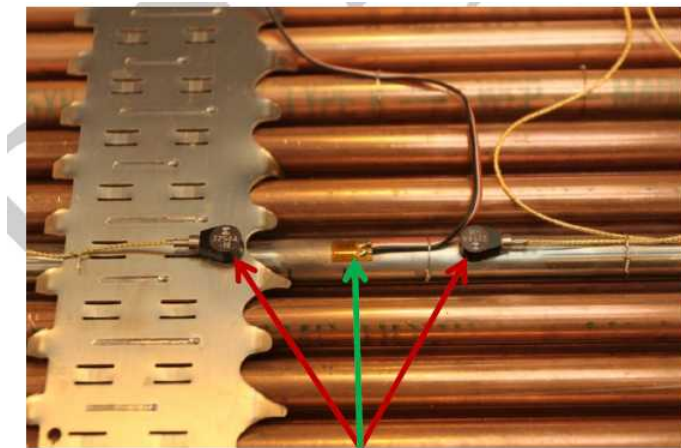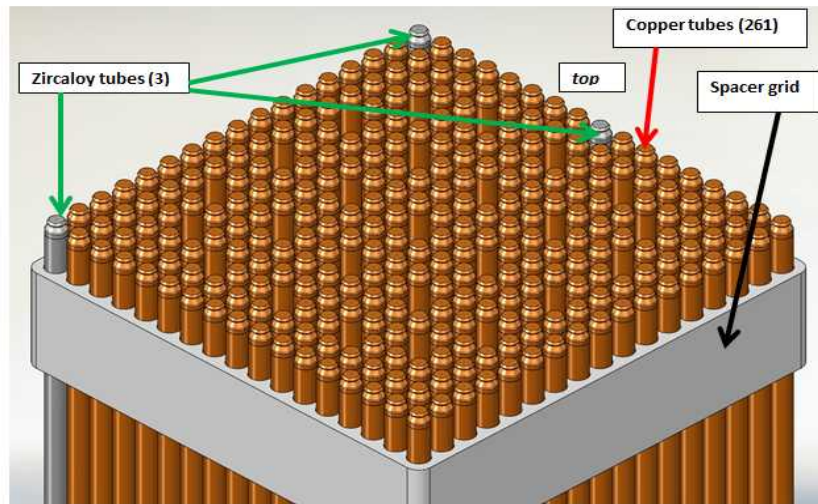

Figure 2. Diagram of Zircaloy-4 rods instrumented for the tests (top) and instrumentation on the actual assembly (bottom). The Zircaloy-4 rod shows as silver against the copper rods.

Shaker

The shaker used for the tests was a MB Dynamics C220 base-isolated electrodynamic shaker system located in the Sandia Experimental Environmental Simulation Organization's Vibration and Acoustics Laboratory. The shaker has a 4-ft shaker head diameter. A 4-ft by 5-ft expander head was mounted onto the shaker head (Figure 3). Capabilities of the shaker include: 10-2,000 Hz sine/random, 30,000 lbs. force, 86 g peak, 45 in./sec velocity, and 2-in. peak-to-peak displacement.
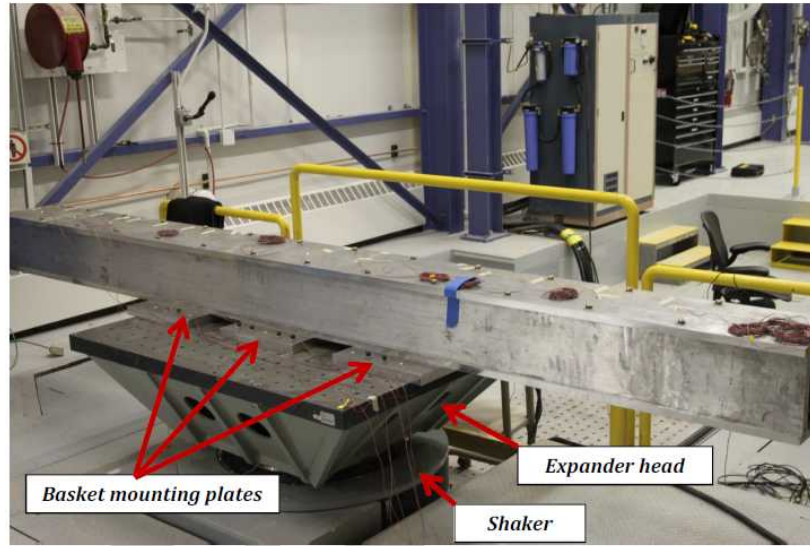
Figure 3. Basket containing assembly on the shaker.

Test input specifications

Input for the shaker was derived from data in "Shock and Vibration Environments for a Large Shipping Container During Truck Transport (Part II)", NUREG/CR-0128 (SAND Report 78-0337), 1978. (Referenced in *Section 2.5.6.5 Vibration* in NUREG-1609, "Standard Review Plan for Transportation Packages for Radioactive Material"). Key details from NUREG/CR-0128 are:

- Vibration and shock data were measured by accelerometers over a 700-mile journey. Two tests, two casks.
- 56000-pound cask and 44000-pound cask (SAND77-1110).
- Measurements were taken on the external body of the casks.
- Speeds ranged from 0 to 55 mph.

Using the most conservative data from this report, the shaker simulated the vibration and shock experienced by the casks during normal transport. Figure 4 shows the random vibration test specification input to the shaker control system and applied to the basket/assembly. Table 2 lists the corresponding breakpoints.
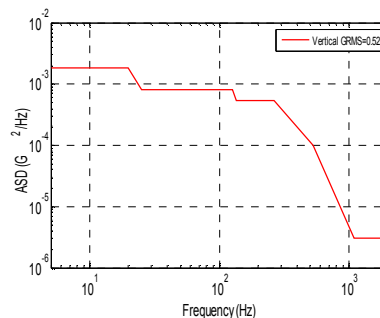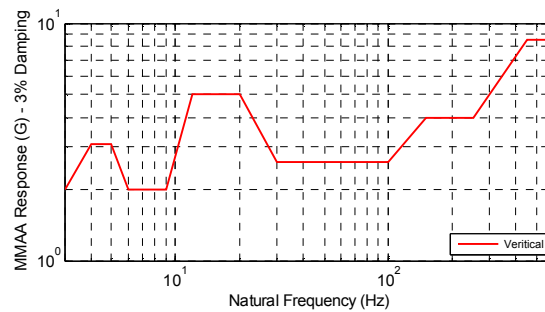

Figure 4. Random vibration test specification

Table 2. Vibration Breakpoints

Frequency (Hz)	(g²/Hz)
5	1.8e−3
20	1.8e−3
25	8.0e−4
125	8.0e−4
135	5.5e−4
265	5.5e−4
530	1.0e−4
1,100	3.0e−6
2,000	3.0e−6

Figure 5 shows the recommended shock test specification. Table 3 lists the corresponding breakpoints.

Figure 5. Recommended Shock Test Specification.

Table 3. Reference Shock Breakpoints

Frequency (Hz)	g
3	2
4	3.1
5	3.1
6	2
9	2
12	5
20	5
30	2.6
100	2.6
150	4
250	4
450	8.5
600	8.5

Test sequence
A total of 11 valid tests, six duplicative vibration tests and five duplicative shock tests, of the basket/assembly unit were performed on the shaker April 30 and May 1, 2013. Frequencies input for the shock tests were limited to a lower bound of 4 Hz.

RESULTS
A segment of the time-history data for a shock and vibration test in units of micro-strain v. time for all of the strain gages are shown in Figure 6. Note the magnitude of the peak strains.
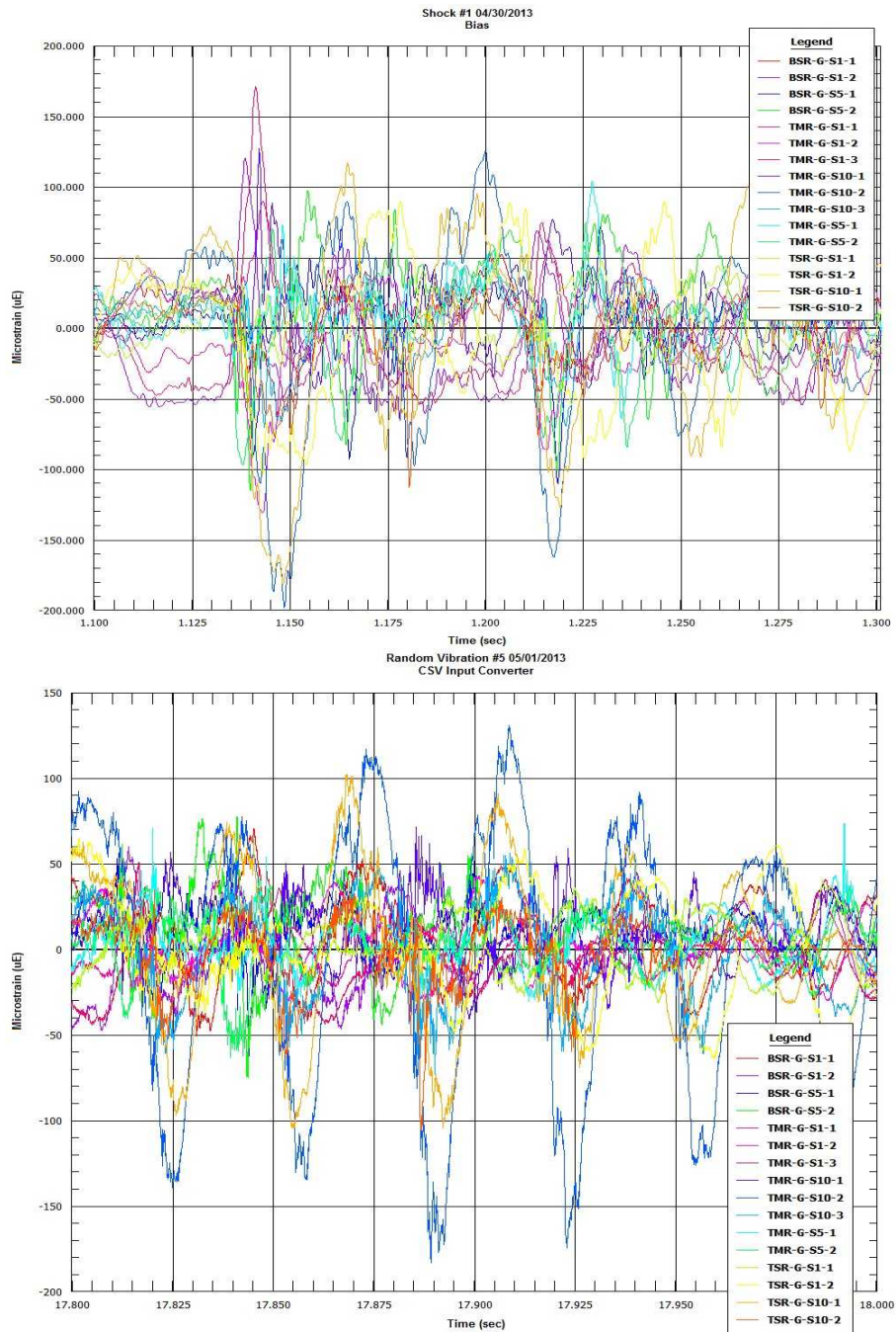
Figure 6. Micro-strain *v.* time for a shock and vibration test for all strain gages

Magnitude of Strains

Tables 4 and 5 present micro-strain and acceleration data recorded for each instrument. There was very little difference between strains measured on the rods due to shock loadings or vibration loads.

Table 4. Strains measured at each strain gage for a shock test

Rod Location	Assembly Span	Position on Span	Maximum Strain (µin./in.)
Top-middle rod	Bottom-end	Adjacent to spacer grid	90
Top-middle rod	Bottom-end	Mid-span	131
Top-middle rod	Bottom-end	Adjacent to spacer grid	171
Top-middle rod	Mid-assembly	Adjacent to spacer grid	104
Top-middle rod	Mid-assembly	Mid-span	97
Top-middle rod	Top-end	Adjacent to spacer grid	127
Top-middle rod	Top-end	Mid-span	199
Top-middle rod	Top-end	Adjacent to spacer grid	70
Top-side rod	Bottom-end	Adjacent to spacer grid	54
Top-side rod	Bottom-end	Mid-span	107
Top-side rod	Top-end	Mid-span	117
Top-side rod	Top-end	Adjacent to spacer grid	113
Bottom-side rod	Bottom-end	Mid-span	62
Bottom-side rod	Bottom-end	Adjacent to spacer grid	121
Bottom-side rod	Mid-assembly	Adjacent to spacer grid	110
Bottom-side rod	Mid-assembly	Mid-span	115
		Average of All Strain Gages	**112**
		Average Top-middle Rod	124
		Average Top-side Rod	98
		Average Bottom-side Rod	102
		Average Bottom-end Span	105
		Average Mid-assembly Span	107
		Average Top-end Span	125
		Average Mid span	118
		Average Adjacent to Spacer Grid	107

Table 5. Strains measured at each strain gage for a vibration test

Maximum Strains, Average Strains ($\mu\varepsilon_{RMS}$), and Average Peak Strains ($\mu\varepsilon_{peak}$) on Zircaloy Fuel Rods Random Vibration Test #5

Rod Location	Span	Position on Span	Maximum Strain (µin./in.)	Average ($\mu\varepsilon_{RMS}$) (µin./in.)	Average ($\mu\varepsilon_{peak}$) (µin./in.)
Top-middle	Bottom-end	Adjacent to spacer grid	70	19	27
Top-middle	Bottom-end	Mid-span	75	21	30
Top-middle	Bottom-end	Adjacent to spacer grid	81	19	27
Top-middle	Mid-assembly	Adjacent to spacer grid	145	15	21
Top-middle	Mid-assembly	Mid-span	80	19	27
Top-middle	Top-end	Adjacent to spacer grid	98	14	20
Top-middle	Top-end	Mid-span	183	42	59
Top-middle	Top-end	Adjacent to spacer grid	74	16	23
Top-side	Bottom-end	Adjacent to spacer grid	60	13	18
Top-side	Bottom-end	Mid-span	128	26	37
Top-side	Top-end	Mid-span	153	41	58
Top-side	Top-end	Adjacent to spacer grid	113	15	21
Bottom-side	Bottom-end	Mid-span	74	17	24
Bottom-side	Bottom-end	Adjacent to spacer grid	71	19	27
Bottom-side	Mid-assembly	Adjacent to spacer grid	106	11	16
Bottom-side	Mid-assembly	Mid-span	92	13	18
		Average All Strain Gages	**100**	**20**	**28**
		Average Top-middle Rod	101	21	30
		Average Top-side Rod	114	24	34
		Average Bottom-side Rod	86	15	21
		Average Bottom-end Span	80	19	27
		Average Mid-assembly Span	106	15	21
		Average Top-end Span	124	26	37
		Average Mid-span	112	26	37
		Average Adjacent to Spacer Grid	91	16	23

The maximum strain on a fuel rod measured during three shock shaker tests listed in Table 4 was 213 µin./in. (µm/m) which was at the mid-span of Span 10 of the top-middle rod during Shock Test #2. Span 10 is one of the longer spans located at the top-nozzle end of the assembly.

For Shock Tests #1, #2, and #5 the absolute value of the average maximum micro-strain for all the strain gages was 99 μin./in. (μm/m).

The maximum strain on a fuel rod measured during three vibration tests listed in Table 5 was 207 μin./in. (μm/m) which was again at the mid-span of Span 10 of the top-middle rod during Random Vibration Test #4. For Random Vibration Tests #4, #5, and #6 the absolute value of the average maximum micro-strain for all the strain gages was 91 μin./in. (μm/m).

The results suggest that failure of the rods during NCT is unlikely due to a strain- or stress-based failure mechanism. The applied strains on the rods and the corresponding applied stresses may be too low relative to the strength of the cladding to cause failure in the absence of cracks. Further work is underway in other DOE programs to assess Zircaloy-4 performance based on inelastic, brittle fracture material property conditions.

The stresses corresponding to the maximum experimentally measured strains are approximately 3 ksi (20.6 MPa) as shown in Figure 7. The figure is a plot of the elastic portion of the stress-strain curves for unirradiated and low-burnup and high-burnup Zircaloy-4. The figure indicates just how low the magnitude of the strains and corresponding stresses were on the rods relative to the elastic limit of unirradiated and irradiated Zircaloy-4. Even with considering the axial stress offset due to internal pressure in irradiated Zircaloy-4 rods, estimated to be approximately 6 ksi (41 MPa), the applied stresses to the rod would be still low relative to the yield strength.
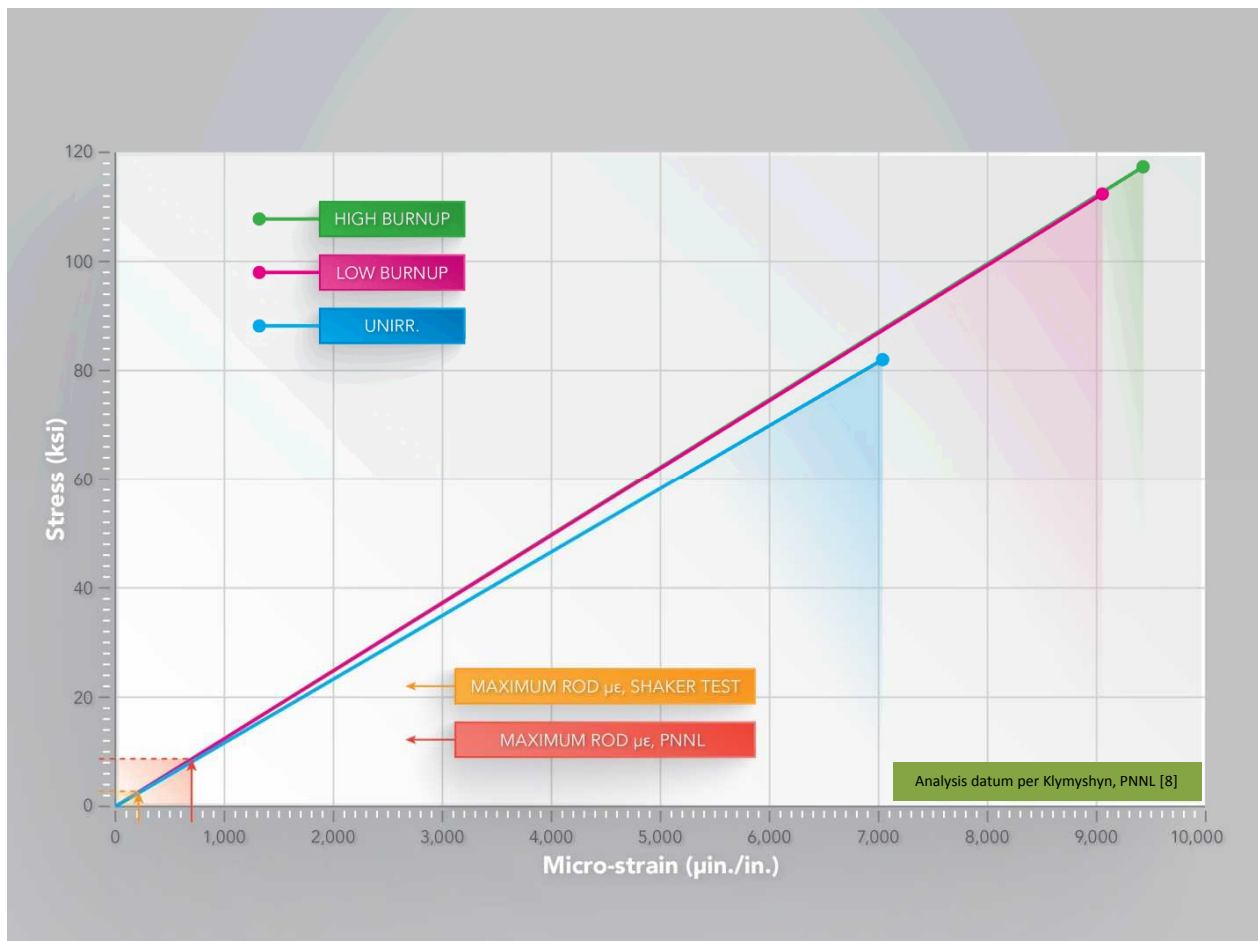

Figure 7. Elastic portion of stress—strain curve for Zircaloy-4 [7], unirradiated, 100°F; low burnup, 250°F; and high burnup, 250°F.

Figure 8 indicates that the desired inputs for the shock and vibration tests were achieved as measured by input/control accelerometer on the shaker.
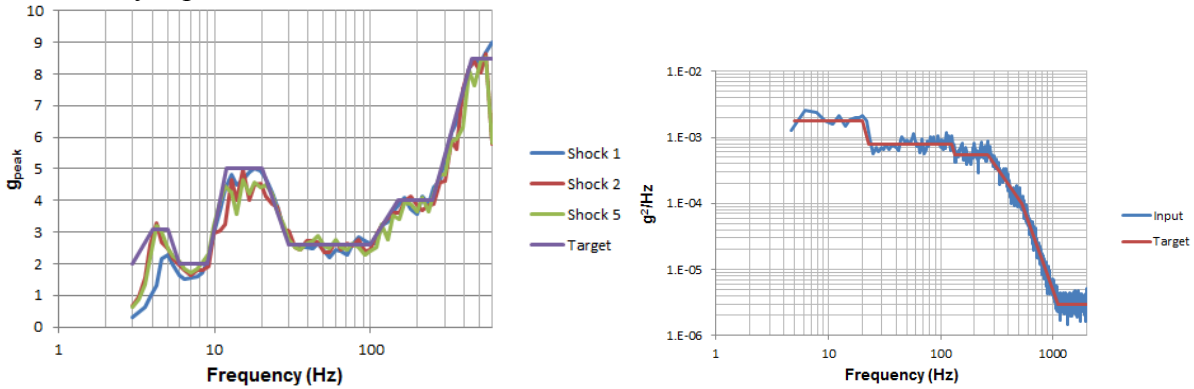

Figure 8. Input/control accelerometer response for shock (left), g *v*. Hz, and vibration (right), g^2/Hz *v*. Hz, relative to the desired target spectra.

Figure 9 show the acceleration power spectral density, g^2/Hz *v*. Hz, of the assembly, per the accelerometers on the central control rod, and the basket.
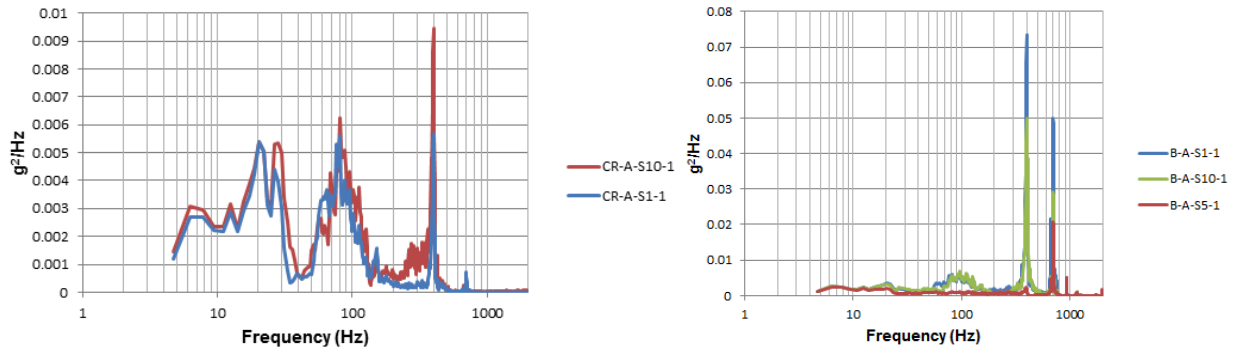
Figure 9. Control rod and basket acceleration power spectral density, g^2/Hz *v*. Hz.

Figure 10 shows the response of the top-middle Zircaloy-4 rod at the long span between spacer grids adjacent to the bottom end of the assembly for a vibration test.
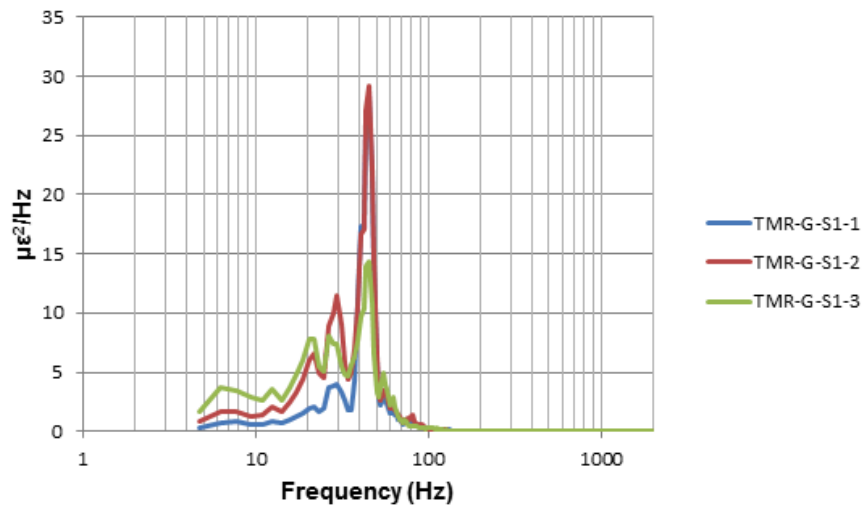
Figure 10. Power spectral density, μɛ^2 *v*. Hz, for the top-middle Zircaloy- 4 during a vibration test

Comparison of Duplicative Test Data
Table 6 compares the maximum strains measured at all locations for Shock Tests #1, #2, and #5 and Random Vibration Tests #4, #5, and #6. This comparison confirms that test results were nearly identical from test to test. For example, the absolute values of the maximum micro-strains measured by the strain gage denoted TM-10-2 for Shock Tests #1, #2, and #5 were 199 µε, 213 µε, and 184 µε; the absolute values of the maximum micro-strains measured by the strain gage denoted TM-10-2 for Random Vibration Tests #4, #5, and #6 were 207 µε, 183 µε, and 172 µε.

Table 6. Comparison of strains for duplicative vibration and shock tests

Gage	Vibration #4		Vibration #5		Vibration #6		Shock #1		Shock #2		Shock #5	
	Max	Min	Max	Min	Max	Min	Max	Min	Max	Min	Max	Min
TM-1-1	69	−60	70	−59	65	−56	90	−46	91	−49	64	−43
TM-1-2	69	−74	67	−75	64	−77	48	−130	56	−119	63	−119
TM-1-3	73	−64	81	−65	71	−57	172	−53	138	−84	148	−75
TM-5-1	156	−66	145	−57	145	−61	104	−64	90	−83	114	−61
TM-5-2	61	−82	70	−80	64	−97	75	−97	99	−88	89	−119
TM-10-1	90	−55	98	−48	83	−47	127	−66	91	−62	107	−77
TM-10-2	138	−207	131	−183	121	−172	126	−199	169	−213	101	−184
TM-10-3	74	−89	67	−74	62	−76	53	−70	69	−71	42	−80
TS-1-1	55	−41	60	−40	70	−45	53	−36	71	−42	85	−67
TS-1-2	97	−122	89	−128	93	−105	107	−110	114	−139	134	−150
TS-10-1	110	−143	113	−153	101	−146	118	−181	130	−153	149	−198
TS-10-2	45	−113	42	−113	45	−106	35	−112	42	−119	45	−115
BS-1-1	67	−69	74	−61	46	−67	55	−62	74	−70	61	−81
BS-1-2	68	−72	71	−58	62	−56	121	−60	116	−74	85	−75
BS-5-1	65	−108	106	−94	70	−97	71	−111	56	−102	60	−120
BS-5-2	94	−98	90	−92	94	−105	97	−115	88	−111	94	−91

Fracture Mechanics Analysis Based on Stresses from Test Data and Analyses
The strain data measured during the tests, for shock and vibration loadings, suggest that the axial strains on the rod—and the corresponding applied stresses—are very low in relation to the elastic limit of unirradiated Zircaloy-4 and the estimated elastic limits for low-burnup and high-burnup Zircaloy-4. This suggests that cladding will not fail during NCT via strain- or stress-based failure criteria (Figure 7).

Irradiation of Zircaloy-4 increases the yield strength of the material with little effect on the elastic modulus. The ductility of high-burnup Zircaloy-4 cladding is no doubt degraded meaning that once the yield limit is reached in high-burnup cladding, there will be little or no plasticity—brittle fracture could occur at the yield limit or below. However, the stresses derived from the strains (and associated stresses) measured in the shaker tests are so low that there is a large margin between the applied stresses and the Zircaloy-4 yield strength.

Cladding could fail via a fracture mechanics-based criterion, however. Brittle fracture can occur at any stress below the yield limit in cladding containing damage or flaws, or that develops flaws under fatigue loading. Limited data, some derived from models, suggests a degradation of the fracture toughness of high-burnup Zircaloy-4. In the presence of a crack in the cladding of sufficient size, fracture could occur at relatively low stresses.

An evaluation of the stresses required to cause fracture in the presence of cracks in high-burnup cladding of various sizes was made. These evaluations required an estimate of the fracture toughness, K_{Ic}, of high-burnup Zircaloy-4. Data for the fracture toughness of Zircaloys is discussed in References [7] and [9].

In order to calculate the stress or crack size required to cause fracture of the cladding, equations relating the applied stress intensity, K_I, the crack size, and the applied stress are used. When the applied stress intensity, K_I, exceeds the fracture toughness, K_{Ic}, fracture at the crack tip occurs. A circumferential crack is the most likely to cause fracture in the presence of axial, bending stresses such as those experienced by cladding.

The expression used for the calculations was:

$$K_I = Y\sigma_b\sqrt{(\pi a)}, \text{ where } Y = 1, \sigma_b = \text{applied bending stress [10]}$$

The Zircaloy-4 rods have a wall thickness, t, of 0.0225 inches (0.57 mm). Semi-elliptical circumferential surface cracks with $a/2c = 1/6$ were assumed, where "a" is the crack depth at the deepest point and "2c" is the length of the crack. The assumed applied stress was 3 ksi (20.6 MPa) which corresponded to the maximum strain measured during the shaker tests. The calculations also assumed through-wall flaws of varying depth, $a/t = 0.1$, 0.25, and 0.5. Table 7 presents results of the applied stress intensities for the maximum applied stresses tests for a range of crack sizes.

Table 7. Estimated applied stress intensities at the tip of circumferential flaws in the cladding of a fuel rod subjected to the experimentally measured maximum stress, 20.6 MPa

Crack depth/Zircaloy-rod wall thickness	Applied stress intensity at crack tip, (MPa-√m)	Lower bound Zircaloy-4 fracture toughness, (MPa-√m)
0.10	0.3	
0.25	0.4	20 - 30
0.50	0.6	

The calculated applied stress intensities are low relative to even a lower bound fracture toughness for Zircaoly-4 and crack depths up to half the clad wall thickness; the fracture toughness of Zircaloy-4 significantly exceeds the applied stress intensities calculated for the stress levels measured for the shaker tests. The resulting implication is that the margin against failure in the presence of a crack on the fuel cladding due to a fracture mechanics-based failure mechanism may be acceptable for the stresses measured by the shaker tests that simulate those expected during normal conditions of transport. The measured strains are very low; it would take a significant preexisting flaw in cladding, and/or significantly degraded fracture toughness, and/or large numbers of cycles under these strains for these strains to be of real concern. This issue should be more thoroughly examined, however, particularly by means of generating additional fracture toughness data on high-burnup Zircaloy-4 and assessments of the sizes of potential cracks in cladding.

CONCLUSION AND FUTURE PLANS

The strains measured in the shaker test program were in the micro-strain levels – well below the elastic limit for either unirradiated or irradiated Zircaloy-4.

Based upon the test results, which simulated normal vibration and shock conditions of truck transport, strain- or stress-based failure of fuel rods during normal transport seems unlikely. Additional testing – shaker and high burnup Zircaloy rod – and additional finite elements analyses are recommended.

Future plans for measuring strains on an assembly are to 1) perform tests on the assembly/basket test unit on the Sandia shaker using rail vibration and shock inputs; 2) perform tests on the assembly/basket test unit on a seismic shaker down to 2 Hz using truck and rail vibration and shock inputs; and 3) instrument an assembly for actual over-the-road testing.

REFERENCES
[1] Code of Federal Regulations, Title 10, Part 71, "Packaging and Transportation of Radioactive Material."
[2] "Regulations for the Safe Transport of Radioactive Material," Specific Safety Requirements No. SSR-6, International Atomic Energy Agency, 2012.
[3] Standard Review Plan for Transportation Packages for Radioactive Material, NUREG-1609, US Nuclear Regulatory Commission.
[4] Magnuson, Cliff F., "Shock and Vibration Environments for Large Shipping Container During Truck Transport (Part II)," SAND78-0337 and NRC NUREG/CR-0128, May 1978; and Magnuson, Cliff F., "Shock and Vibration Environments for Large Shipping Container During Truck Transport (Part I)," SAND77-1110, September 1977.
[5] Magnuson, C.F., "Shock Environments for Large Transport Containers During Rail-Coupling Operations," Sandia National Laboratories, Albuquerque, NM, SAND79-2168, NUREG/CR-1277, June 1980.
[6] Nicholas Klymyshyn, "Shaker Table Modeling Progress Report," #UFDCST-120927-1, Pacific Northwest National Laboratory, September 2012.
[7] Ken Geelhood and Carl Beyer, "Used Nuclear Fuel Loading and Structural Performance Under Normal Conditions of Transport – Supporting Material Properties and Modeling Inputs," Pacific Northwest National Laboratory, US Department of Energy Used Fuel Disposition Campaign Report FCRD-UFD-2013-000123, March 16, 2013.
[8] Nicholas Klymyshyn, Scott Sanborn, Harold Adkins, and Brady Hanson, "Fuel Assembly Shaker Test Simulation," FCRD-UFD-2013-000168, Pacific Northwest National Laboratory, May 30, 2013.
[9] Rashid, Y.R., R.O. Montgomery, W.F. Lyons, "Fracture Toughness Data for Zirconium Alloys – Application to Spent Fuel Cladding in Dry Storage," Electric Power Research Institute Technical Progress Report 1001281, January 2001.
[10] FITNET Annex A, "Stress intensity factor (SIF) solutions," *ocw.unican.es/ensenanzas-tecnicas/.../otros.../soluciones_fit__fitnet_.pdf*, May 2006.